J. Water Environ. Nanotechnol., 9(1): 55-72 Winter 2024

ORIGINAL RESEARCH PAPER

Natural biodegradable low-cost Lablab purpureus husk as chromatrap for removal of three hazardous organic cationic dyes from water: Waste to wealth and column elution approach

Sumathi Harohally Paramesh[1], Veerendra Shetty Ananthpur[1], and Nagaraju Rajendraprasad[1]*

[1] PG Department of Chemistry, JSS College of Arts, Commerce and Science, A Research Centre Recognized by University of Mysore, Mysuru-570 25, Karnataka, India

Received: 2023-09-21 Accepted: 2023-11-18 Published: 2024-01-31

ABSTRACT

Novel results in this study showcase the utilization of sunlight-dried, ground *Lablab purpureus* husk (LLPh), treated with water and alkali, as a highly efficient bio-adsorbent for the removal of cationic dyes from aqueous solutions. Methylene blue (MB), malachite green (MG), and crystal violet (CV) were effectively adsorbed onto NaOH-activated LLPh (NaOH-LLPh) as bio-adsorbent. Employing the Chromatrap method within a column, successfully removed these dyes, while the surface morphology of the bio-adsorbent was elucidated through scanning electron microscopy (SEM) analysis. FTIR spectrometric data revealed valuable insights into the extent of adsorption. The impact of factors including adsorbate concentration, adsorbent dose, pH, contact time, and flow rate on the adsorption process was systematically studied and optimized. Up to 1000 µg/mL of MB and MG and 50 µg/mL of CV were found to be effectively removed by adsorption at pH 4-5, 3, and 2, respectively, at the flow rate of 1 mL/min. The results of kinetic studies and adsorption isotherms of the above-mentioned dyes indicate that all three dyes follow the pseudo-second-order kinetics. The adsorption of MB and MG are well fitted with the Langmuir isotherm model. The other dye CV suits with the Freundlich isotherm model. Based on the results, NaOH-LLPh, as an inexpensive and eco-friendly adsorbent, is suitable for the removal of cationic organic dyes from aqueous samples.

Keywords: *Lablab Purpureus Husk, Chromatrap, Methylene Blue, Malachite Green, Crystal Violet, Scanning Electron Microscope.*

How to cite this article

Paramesh S. H., Ananthpur V. S., Rajendraprasad N., Natural biodegradable low-cost Lablab purpureus husk as chromatrap for removal of three hazardous organic cationic dyes from water: Waste to wealth and column elution approach. J. Water Environ. Nanotechnol., 2024; 9(1): 55-72. DOI: 10.22090/jwent.2024.01.04

INTRODUCTION

Dyes are widely used to colorize the products in textile, leather, paper, wood, wool, pharmaceutical, cosmetic as well as in food industries [1, 2]. The effluents discharged straight into the water bodies from these industries are largely responsible for endangering aquatic life and creating carcinogenic effects. Long-term contact with dyes causes itching and irritation in humans; however, children are affected more quickly [3]. Thus, it is inevitable to make sure that industrial effluent is rendered less contaminated by removing harmful compounds by utilizing removal processes. Various techniques, including physical, chemical, and biological methods, can be employed to address significant contaminants such as organic compounds or dyes. The utilization of nanocatalysts [4-6], Fenton catalysts [7], and artificial neural networks [8] for eliminating these pollutants has gained increasing attention in research. Conversely, adsorption is on the rise in popularity due to its efficiency, environmental friendliness, and straightforward interpretability [9].

Methylene blue (MB), malachite green (MG) and crystal violet (CV) are familiar

* Corresponding Authors Email: *prasadtnpur@gmail.com*

This work is licensed under the Creative Commons Attribution 4.0 International License.
To view a copy of this license, visit http://creativecommons.org/licenses/by/4.0/.

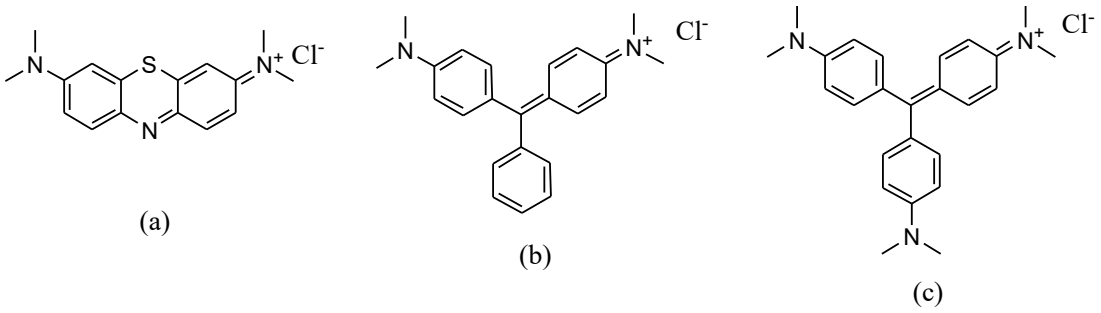

Fig. 1. Chemical structures of (a) MB, (b) MG, and (c) CV

with the IUPC names: [7-(dimethyl- amino) phenothiazin-3-ylidene]-dimethyl-azanium, chloride (Fig. 1a), [4-[[4-(dimethylamino) phenyl]-phenylmethylidene]cyclohexa-2,5-dien-1-ylidene]- dimethyl-azanium, chloride (Fig. 1b) and tris(4-(dimethylamino)phenyl)methylium chloride (Fig. 1c), respectively.

Among the many synthetic dyes, MB, MG, and CV are the most widely used organic cationics in the textile and pharmaceutical industries. The effluents containing trace levels of these organic cations must be eliminated to reduce the nocuous properties of water [10, 11].

Bio-adsorbents have garnered considerable attention in recent years for their effectiveness in removing various contaminants from wastewater [12]. These materials, derived from natural sources like plants, agricultural waste, and microorganisms, offer distinct advantages such as affordability, abundant availability, biodegradability, and environmental friendliness [12]. Researchers have explored a broad spectrum of bio-adsorbents and devised innovative strategies for pollutant removal. Some of the adsorbents investigated for MB removal include activated carbon from jatropha husk [13], magnetic peanut husk [14], phosphoric acid-treated balanites aegyptiaca seed husk powder [15], sodium hydroxide-treated rice husk [16], mentha plant waste [17], rice husk ash [18], nanoparticles synthesized from rice husk [19], oxalic acid-modified rice husk [20], rice husk biochar [21], porous carbon material from rice husk [22], and neem (Azadirachta indica) leaves [23]. Furthermore, activated carbon from coffee husk [24], zinc chloride-modified hazelnut husk [25], and lemongrass husk [26] were explored for MB removal. Additionally, Hydnocarpus pentandra fruit peel charcoal [27], coffee husk biochar [28], dried biomass of haloxylon recurvum plant stems [29], lathyrus sativus husk [30], magnetic rice husk ash [31], and biochars from rice husk, cow dung, and domestic sludge were effectively employed, achieving approximately 90% MB removal. Corn plant husks [33], sawdust of Gmelina arborea roxb [34], and palm oil mill effluent waste-activated sludge were also utilized for MB removal [35].

Numerous adsorbents for MG removal, as reported by different researchers, include highly porous quinoa husk [36], sodium carbonate-treated rice husk [37], raw and activated forms of Gibto (Lupinus albus) seed peel powder [38], activated carbon from groundnut shell powder [39], typha australis leaves [40], durian seed-based activated carbon [41], rice husk, Thespesia Populnea bark, Calatropis gigantic bark, corn cob, neem bark, mango bark, root powder of water hyacinth (Eichhornia crassipes), Araucaria cookii bark, and seaweed Enteromorpha [42], hydrochloric acid-treated sphagnum peat moss [43], jackfruit leaf powder [44], root powder of chemically modified activated walnut shell powder [45], garlic root powder [46], luffa aegyptica peel powder [47], Cocos nucifera husk [48], potato peel, and neem bark [49]. Additionally, durian peel-activated carbon [50], date-stone activated carbons [51], xanthate wheat bran [52], activated carbon from teak wood waste [53], clove leaves powder [54], sawdust waste from Gmelina arborea [34], EDTA-modified groundnut husk [55], Rhizophora mucronata stem-barks [56], and lemongrass leaf powder [57] were explored for MG removal.

A few reports described the procedures for the removal of CV includes, including methods using lignocellulosic agricultural waste [58], Eichhornia charcoal [59], NaOH-modified rice husk [60, 61], the activated carbon of African star apples [62], red algae Gelidium pusillum [63], phyllanthus emblica fruit powder [64], olive pomace [65], activated carbon of the coconut shell [66], tartaric acid modified Holarrhena antidysenterica and

Table 1. Comparison of the proposed work with similar reported works

Dye	Adsorbent used	Adsorbent dose	Methodology and experimental conditions	Adsorption Capacity	Comments	Reference No.
MB	Phosphoric acid-treated Balanites aegyptiaca seed husk powder	0.02-0.12 g/20 mL	Batch adsorption method; Shaking speed: 150 to 300 rpm, contact time: 0-120 min, initial MB concentration: 100-300 mg/L, solution temperature: 25-45 C and initial solution pH: 4-13	97%	Applicable to low-concentration solutions, batch adsorption up to 120 min	15
	NaOH-modified rice husk	2–6 g/l	Batch adsorption method; pH: 7–10, initial concentration of dye: 25–125 mg/l	97.66%	Applicable to low-concentration solutions, batch adsorption up to 120 min	16
	Oxalic acid-modified rice husk	3 g/L	Batch adsorption method; pH: 7, mechanical shaking for 480 min for equilibration	19.77 mg/g	A shaking time of 480 min required	20
	Corn plant husk	2 g/L	Batch adsorption method; pH: 6; Dye concentration: 20 – 100 mg/L	Upto 93.6%	Less efficient method	33
	NaOH-activated Lablab purpureus husk	0.25 g	Column adsorption and elution approach; pH: 4-5; Temperature: Room Temperature; Flow rate: 1mL /min Concentration: Upto 1000 mg/L	Upto 98%	More efficient. Rapid equilibration approach. Novel column adsorption method is used.	Present work
MG	NaOH-treated rice husk	10 g/L	Batch adsorption method; Dye concentration: Upto 200 mg/L; pH: 7-7.5; Equilibration time: 90 min	Upto 98%	Longer equilibration time is required	37
	Coconut husk	20-50 g/L	Batch adsorption with mechanical shaker; pH: 3-7; Time: 80- 300 minutes	Upto 92.81%	Longer equilibration time is required	48
	a) Groundnut husk b) EDTA-modified groundnut husk	0.2 g	Batch adsorption method; Dye concentration: Upto 50 mg/L; pH: 7-8; Equilibration time: 50 min	a) 78.6% b) 92.4%	Less efficient and longer equilibration time	55
	NaOH-activated Lablab purpureus husk	0.25 g	Column adsorption and elution approach; pH: 3; Temperature: Room Temperature; Flow rate: 1mL /min Concentration: Upto 1000 mg/L	Upto 98.64%	More efficient. Rapid equilibration approach. Novel column adsorption method is used.	Present work

NA: Not available

Citrullus colocynthis husks [67] and Urtica dioica leaf powder [68].

Furthermore, adsorbents derived from Carnauba straw [69], Eucalyptus leaves [70], and amine-functionalized chitosan [71] were identified as effective mediums for both CV and MB adsorption.

In the review of literature, methods to remove MB, MG, and CV were found using a variety of husks as adsorbents. The details about the husk, adsorbent dose, and experimental parameters are given in Table 1. Most of the methods follow a batch adsorption process to trap the dye. Almost in each case, a longer equilibration time for adsorption was noticed.

Although numerous researchers employed different materials to remove MB, MG, and CV, none of them documented the utilization and effectiveness of *Lablab Purpureus* husk (LLPh). *Lablab Purpureus* (Haycinth beans) is utilized as

Table 1. Comparison of the proposed work with similar reported works - (Continue)

Dye	Adsorbent used	Adsorbent dose	Methodology and experimental conditions	Adsorption Capacity	Comments	Reference No.
CV	NaOH-modified rice husk	NA	Laboratory-scale fixed-bed column approach used. A two-level three-factor (2^3) full factorial central composite design is followed Dye concentration (100–200 mg/L^1), flow rate (10 – 30 mL/min), and bed height (5–25 cm)	99.5%	Sophisticated equipment required	60
	NaOH-modified rice husk	0.5 – 5.0 g	Batch adsorption studies were carried out; Dye Concentration: 50 mg/L; Equilibration time: 3h; pH: 7 - 10	Upto 98.17	Longer equilibration time required	61
	Tartaric acid-modified Holarrhena antidysenterica	0.8 g	Batch adsorption method; Contact time: 35 minutes, pH: 5.0, T: 40°C, and Agitation rates: 150 rpm	Upto 97%	Longer equilibration time required	67
	Tartaric acid modified Citrullus colocynthis	1.4 g	Batch adsorption method; Contact time: 40 minutes, pH: 6.0, T: 50°C, and Agitation rates: 150 rpm	Upto 86%	Longer equilibration time required; Less efficient method	
	NaOH-activated Lablab purpureus husk	0.25 g	Column adsorption and elution approach; pH: 2; Temperature: Room Temperature; Flow rate: 1mL /min Concentration: Upto 50 mg/L	Upto 87.98%	More efficient. Rapid equilibration approach. Novel column adsorption method is used.	Present work

NA: Not available

a food in South Asia, East Asia, South East Asia, and East Africa. Since LLPh is the most commonly available and discarded trash, its usage for removing dyes from aqueous samples will elevate the interest of researchers. Out of all the described adsorbents, the LLPh material provides a better adsorption surface for the effective binding of dyes, according to careful examination of the performance. The application of the treatment is neither difficult nor complicated.

Hypothetically, LLPh, when processed by sunlight drying, grinding, and alkali washing, can effectively serve as a bio-adsorbent for the removal of cationic organic dyes, namely, MB, MG, and CV from water. It is expected that NaOH-activated LLPh (NaOH-LLPh) will exhibit significant dye removal capabilities, making it a viable and eco-friendly option for wastewater treatment.

The principle of 'chromatrap', i.e., trapping of dyes in the column using adsorption onto the adsorbent is streamlined in this work for the very first time. This study earnestly endeavors to assess the potency of NaOH-LLPh as a bio-adsorbent for the effective removal of MB, MG, and CV. It also aims to ascertain the optimal operational conditions, encompassing crucial parameters like adsorbate concentration, adsorbent dosage, pH, contact time, and flow rate. Furthermore, it seeks to delve into the kinetic characteristics of dye adsorption and to scrutinize adsorption isotherms, thus unraveling the intricacies of the adsorption mechanism. Notably, this work represents a pioneering effort in this field.

The pioneering application of the Chromatrap principle through column adsorption, employing the cost-effective NaOH-LLPh, marks the novelty of this research. This breakthrough eliminates the requirement for intricate equipment or specialized techniques, thereby making this methodology accessible in a broader sense. This advancement has the potential to elevate its utilization to standard practice in wastewater treatment processes.

Therefore, a smart attempt was made to remove MB, MG, and CV from aqueous solutions using

NaOH-LLPh as a harmless material by column elution approach.

EXPERIMENTAL

Apparatus

The Agilent Cary 60 UV-visible spectrophotometer (Agilent Technologies Ltd, Mumbai, India) was used for all spectrophotometric measurements. Fourier Transform Infrared Spectrometer (FTIR) (Perkin Elmer Instrument, Version 10.7.2, Mumbai, India) was used for all infrared spectral recordings. Scanning Electron Microscope Zeiss (Model EVO LS 15, Germany) with smartSEM™ software was used for the study of the surface morphology of adsorbent before and after adsorption.

Materials

All chemicals utilized in the experiment were of analytical chemical grade. Local distributors provided methylene blue (MB), malachite green (MG), crystal violet (CV), and sodium hydroxide (NaOH) pellets (all from SD Fine Chem Ltd., Mumbai, India). Three water samples were procured from the textile industries of Mysuru city and used for analysis.

Preparation of adsorbent

Lablab purpureus was grabbed from the vegetable market in Mysuru and the husk was meticulously separated and dried under sunshine to ensure total moisture removal. To make raw husk powder, the dried husk was finely pulverized. To remove any dust or undesired elements, the raw husk powder was washed many times with distilled water and then dried under sunlight to produce beneficiated husk powder. It was then treated with a 0.1M NaOH solution. This treatment not only aids in the removal of pigments but also improves the adsorption sites on the adsorbent's surface. The resulting NaOH-activated Lablab pupureus husk (NaOH-LLPh) powder was carefully preserved in a glass jar for later use.

Standard solutions of dyes

By dissolving appropriate weights of chemicals in bi-distilled water, stock standard solutions of MB (3000 µg/mL), MG (3000 µg/mL), and CV (1000 µg/mL) were created. These solutions were employed for elution through the column after adequate dilutions with water.

General procedures

Procedure for column preparation

As adsorbent, 0.25 g of carefully weighed NaOH-LLPh powder was packed in a 25 mL borosilicate glass column. Water was allowed to pass through the column to ensure the absence of any break in the column. Furthermore, a small amount of excess water was left in the column right above the packed adsorbent to prevent the column from splitting.

General Procedure for Dye Removal

With the help of a syringe, a 5 mL of stock solution of each dye (MB and MG: 1000 mg/L; CV: 50 mg/L,) was introduced at a flow rate of 1 mL/min along the sides of the column. The effluent was collected into a small beaker and the absorbance was measured at the corresponding absorption maximum of each dye using a visible spectrophotometer. The concentrations and thus the proportions of dye adsorbed were estimated using the following formula:

$$\%\text{Adsorption} = \frac{D_i - D_f}{D_i} \times 100 \quad (1)$$

where D_i and D_f are the concentrations of dyes before and after adsorption, respectively.

Application to removal of dyes from industrial effluent

A 10 mL portion of industrial effluent was mixed with 10 mL of separate 2000 mg/L standard aqueous solutions of MB, MG, and CV. From this, precisely 5 mL of the solution was drawn into a syringe and then introduced into a column filled with 0.25 g of NaOH-LLPh adsorbent. All within the confines of carefully optimized experimental conditions, the effluent from the column was collected in a beaker, and its absorbance at the respective wavelength of maximum was measured. The procedure has been repeated two more times. The mean percent adsorption of each dye was calculated by using the formula described above.

Characterization of Adsorbent

Recording of FTIR Spectra

The FTIR analysis of adsorbent before and after adsorption was carried out using KBr pellets and recorded in the range from 500 – 4000 cm^{-1}. Different peaks of vibrations were identified and correlated with the functional groups present in the subjected individual samples.

Scanning electron microscopic (SEM) study of adsorbent

The SEM experiment was performed using the instrument with a thermionic emission electron source under variable pressure mode. The optimal images were captured at an accelerating voltage of 10000 V, a working distance of 6500 µm, and an emission current of 99000 nA. The fast scan speed was maintained during the recording of images.

Physicochemical analysis

Moisture content

To determine the moisture content of the NaOH-LLPh, the temperature of the hot air oven was set to a temperature of 105 °C. A thoroughly cleaned crucible containing 1g of the NaOH-LLPh adsorbent was placed in the oven for 4 hours. The crucible was carefully removed and brought to room temperature. The adsorbent was weighed and the moisture content was then calculated using the formula:

$$\text{Moisture Content (MC)} = \frac{M_0 - M_f}{M_0} \times 100 \quad (2)$$

where, M_0 and M_f are the weight of adsorbent before and after heating, respectively.

Ash content

A 1g of NaOH-LLPh adsorbent was weighed carefully and placed in a clean, dry crucible and resided in a muffle furnace maintained at 500°C for 4 hours. It was then taken out of the furnace and placed in a desiccator to cool to room temperature. It was then reweighed. The adsorbent's ash content (AC) was then estimated using the formula:

$$\text{Ash Content (AC)} = \frac{M_s}{M_a} \times 100 \quad (3)$$

where M_a and M_s are the recorded weights of adsorbent before and after furnacing, respectively.

Volatile Matter (VM)

An accurately weighed 1g of the NaOH-LLPh was taken in a crucible and heated in a muffle furnace set to 500°C for 8 minutes. Then, the adsorbent was removed and the Volatile Matter (VM) was calculated by using the formula:

$$\text{Volatile Matter (VM)} = \frac{M_1 - M_2}{M_1} \times 100 \quad (4)$$

where M_1 and M_2 are the initial and final weights of the adsorbent, respectively, in the experiment.

Fixed carbon content (FCC)

It was determined by subtracting the percentage of MC, AC, and VM from 100%, i.e.,

Fixed carbon content (FCC) =100% - (MC+AC+VM) ---------(5)

The experiments were also performed to determine the MC, AC, VM, and FCC of dyes by following the procedure described above for adsorbent.

RESULTS AND DISCUSSION

The LLPh proves to be a promising adsorbent thanks to its anticipated composition, much like other plant materials. It comprises a diverse array of organic compounds, encompassing cellulose, hemicellulose, lignin, and numerous other constituents. Following thorough washing with both alkali and water, all soluble species are effectively eliminated. Consequently, the activated husk, NaOH-LLPh, endowed with a variety of adsorption sites, is expected to exhibit excellent performance in adsorbing dyes, namely, MB, MG, and CV, as demonstrated in this pioneering study.

The adsorbent has been subjected to FTIR and Scanning Electron Microscopic (SEM) studies before and after adsorption to ensure the expected process.

FTIR spectroscopic study

The FTIR spectra of NaOH-LLPh were recorded before and after adsorption. The adsorbent exhibited three distinct absorption peaks at 1023.80, 1609.92, and 3338.67 cm^{-1} (Fig. 2a). These peaks are likely attributed to the C-O and C=C stretching vibrations within the adsorbent. The peak at 3338.67 cm^{-1} is concerned with the stretching vibration of O-H bonds.

The spectrum of the adsorbent after the adsorption of MB is presented in Fig. 2b. Among the total of eight peaks observed, five are significant: around 1096 cm^{-1} for C-S stretching, 1147 cm^{-1} and 1252 cm^{-1} for C-N stretching, and 1337 and 1394 cm^{-1} for C-H bending vibrations of MB.

In Fig. 2c and 2d, absorption peaks at around 1300 and 1400 cm^{-1} are evident, which can be attributed to the presence of C-N stretching and C-H bending vibrations in amine and alkyl groups of MG and CV. Additionally, there are additional peaks in Fig. 2d and they are at 800 cm^{-1} (out-of-plane C-H bending vibrations), approximately 1200-1300 cm^{-1} (C-N stretching), 1550 cm^{-1} (C=C stretching), and around 2800-2900 cm^{-1} (C-H

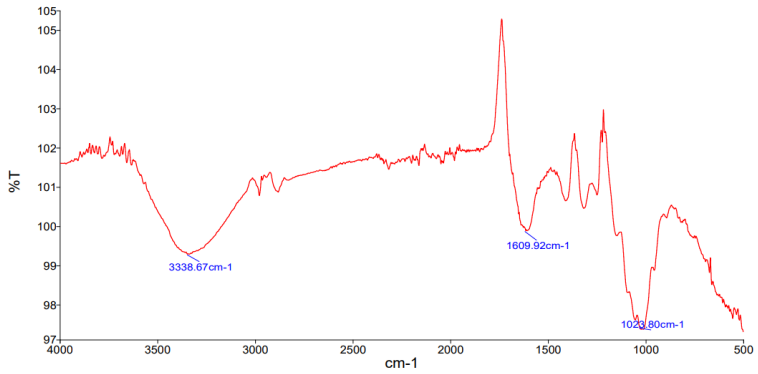

(a)

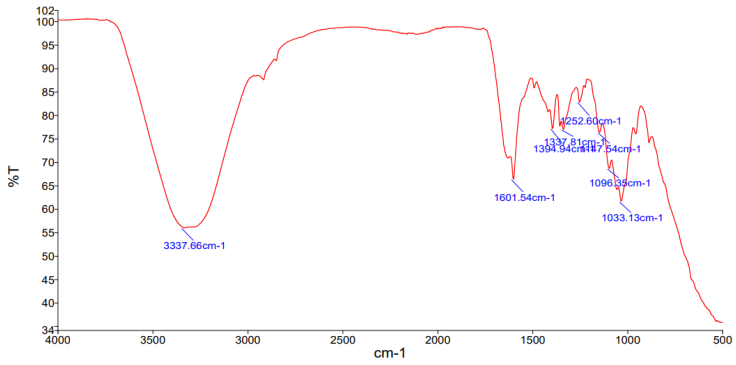

(b)

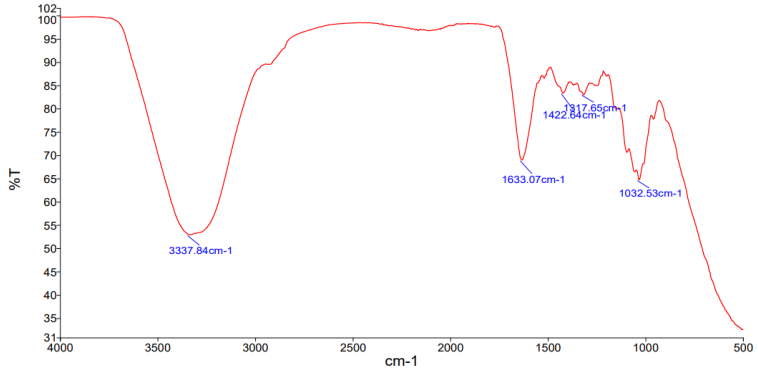

(c)

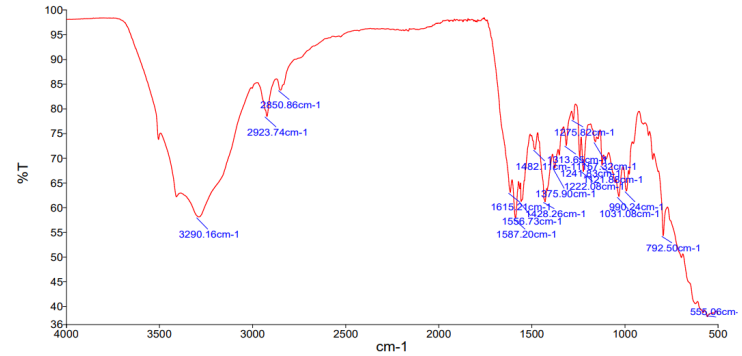

(d)

Fig. 2. FTIR spectra of (a) NaOH activated, (b) MB-, (c) MG - and (d) CV- adsorbed adsorbent

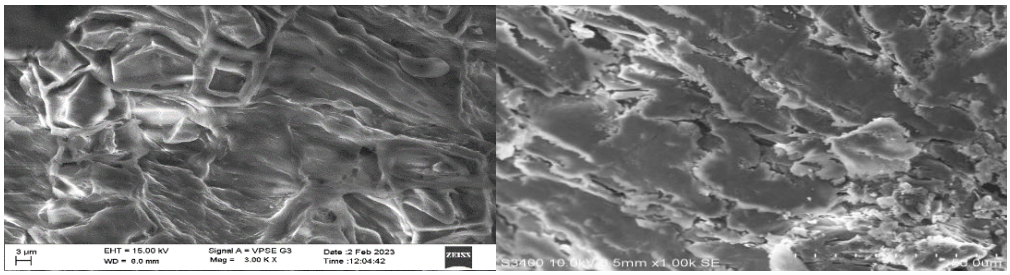

Fig. 3. SEM images captured at an accelerating voltage of 10000 V, a working distance of 6500 µm, and emission current of 99000 nA for a) the activated husk (adsorbent) (3000X) magnification and b) husk after adsorption of dye.

Table 2. Results of the study of physicochemical characteristics of activated *Lablab purpureus* husk

Parameter	MC±SD, %	AC±SD, %	VM±SD, %	FCC±SD, %
Value*	2±0.021	1.27±0.006	93.93±0.87	1.8±0.01

Equipment- MC: Hot air oven; AC: & VM: Muffle Furnace.
Temperature (°C)- MC: 105; AC & VM: 500
Duration- MC & AC: 4 h; VM: 8 min
The mean value of 3 determinations.

Table 3. Physicochemical properties of dyes of study

Property	Value*		
	MB	MG	CV
Melting point (MP), °C	108	164	205
Moisture content (MC), %	15.00	7.00	8.00
Ash content (AC), %	1.00	5.68	1.50
Volatile matter (VM), %	78.07	82.6	86.4
Fixed carbon content (FCC), %	5.93	4.72	4.10

Equipment- MC: Hot air oven; AC: & VM: Muffle Furnace.
Temperature (°C)- MC: 105; AC & VM: 500
Duration- MC & AC: 4 h; VM: 8 min
The mean value of 3 determinations.

stretching). These peaks unmistakably indicate the characteristic presence of CV on the adsorbent.

The identification of specific functional groups on the surface of the NaOH-LLPh provides valuable insights into the molecular interactions and adsorption mechanisms involved in the adsorption of MB, MG, and CV [37, 73].

SEM Analysis of adsorbent

The Scanning Electron Microscopic (SEM) analysis was performed using an acceleration voltage of 10 kV to examine the surface properties and structural attributes of the adsorbent both before and following the adsorption process. The SEM produced crisp images of the NaOH-LLPh at the nanoscale. At high magnification, the photos revealed convolutions, small pores, and up and down surfaces on the adsorbent's surface. The emergence of an exposed surface in Fig. 3a and the subsequent concealment of certain spots, as depicted in Fig. 3b, provided the confirmation of adsorption occurring on the material's sites.

Physicochemical values of adsorbent

The experimental results of MC, AC, VM, and FCC of adsorbent and the dyes are summarised in Tables 2 and 3. As shown in Table 2, it is clear that the NaOH-LLPh exhibited perfect behavior in attracting colors *via* surface phenomena without enduring its destructive pathway after treatment.

Optimization of experimental parameters

The experimental parameters: adsorbent dose, dye concentration, contact time, flow rate, and pH

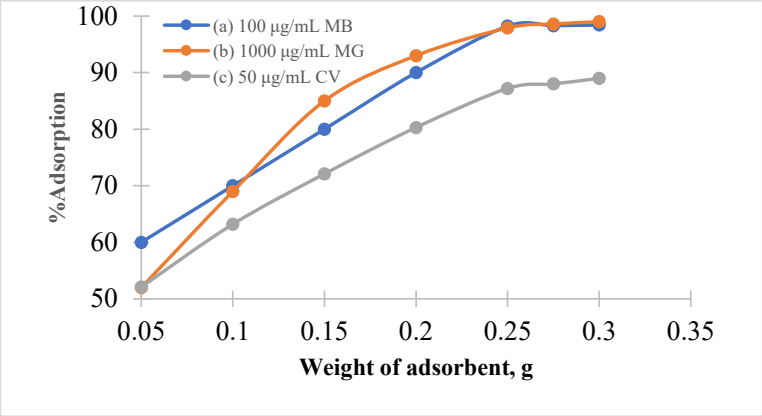

Fig. 4. Plots showing the effect of adsorbent dosage on %adsorption of (a) MB (1000 mg/L), (b) MG (1000 mg/L), and (c) CV (50 mg/L) at volume 5 mL and flow rate of 1 mL/min

were investigated. The optimization was carried out by altering the parameter of interest while holding the others constant.

Adsorbent dose

For each dye, different amounts of the NaOH-LLPh adsorbent material were used. To determine the adsorbent load, the effects of flow rate, adsorption capacity, volume of introduction, and speed of removal were considered. The amount of adsorbent in the column was specifically designed to improve removal efficiency. Thus, of the 0.05 to 0.30 g of material load in the column, the feasible and maximum percentage of dye removal was recorded at 0.25g. As a result, the column was filled with 0.25 g of adsorbent to remove the dyes. The effect of adsorbent dosage on percent adsorption is presented in Fig. 4.

Effect of concentration of dye

To accurately determine the adsorption capacity of the NaOH-LLPh adsorbent the amount of dye that can be adsorbed per unit mass needs to be fixed. Therefore, in evaluating the efficiency of the adsorbent material, in a series of separate experiments, 5 mL aliquots of varied concentrations of MB, MG, and CV dyes were passed through the column filled with NaOH-LLPh to cap the concentrations. The resultant effluent of each case was spectrophotometrically measured at the wavelength maxima of 590, 668, and 624 nm for CV, MB, and MG, respectively. It was discovered that utilizing 0.25 g of NaOH-LLPh, 50 mg/L CV was efficiently removed up to 87.98% as shown in Fig. 5(a-c). Up to 1000 mg/L of both MB and MG were effectively removed to an extent of more than 98% by using the same dose of adsorbent. Concentrations of MB exceeding 1000 mg/L necessitated extended contact times to achieve removal rates exceeding 98%. As a result, the threshold concentration for effective MB removal was established at 1000 mg/L.

Effect of pH on adsorption of dyes

The pH influence on the adsorption of MB, MG, and CV dyes was studied. The experimental results revealed that each dye has a different pH dependence. The pH was adjusted between 2 and 11 for each dye to investigate the effect. Following elution via the column, the corresponding percentage elimination of CV, MB, and MG dyes was computed and the effect was depicted in Fig. 6. According to the experimental data, the highest removal of CV was seen at pH 2, resulting in a removal percentage of 87.98. This may be attributed as at pH 2, CV is likely to be positively charged due to its basic nature. This positive charge facilitates its adsorption onto adsorbents, leading to effective removal. For MB, pH between 4 and 5 resulted in the highest removal rates, reaching >98%. The dye MB exhibits optimal removal between pH 4 and 5 using NaOH-LLPh. The charge and solubility characteristics of MB are conducive to adsorption under slightly acidic conditions. It forms a stable complex with the NaOH-LLPh at this pH range. When it comes to MG dye, pH 3 was shown to be the best level, with a removal rate of 98.64%. This is probably due to similar pH-dependent charge and solubility effects. It is positively charged at lower pH levels, enhancing its adsorption to surfaces of NaOH-LLPh.

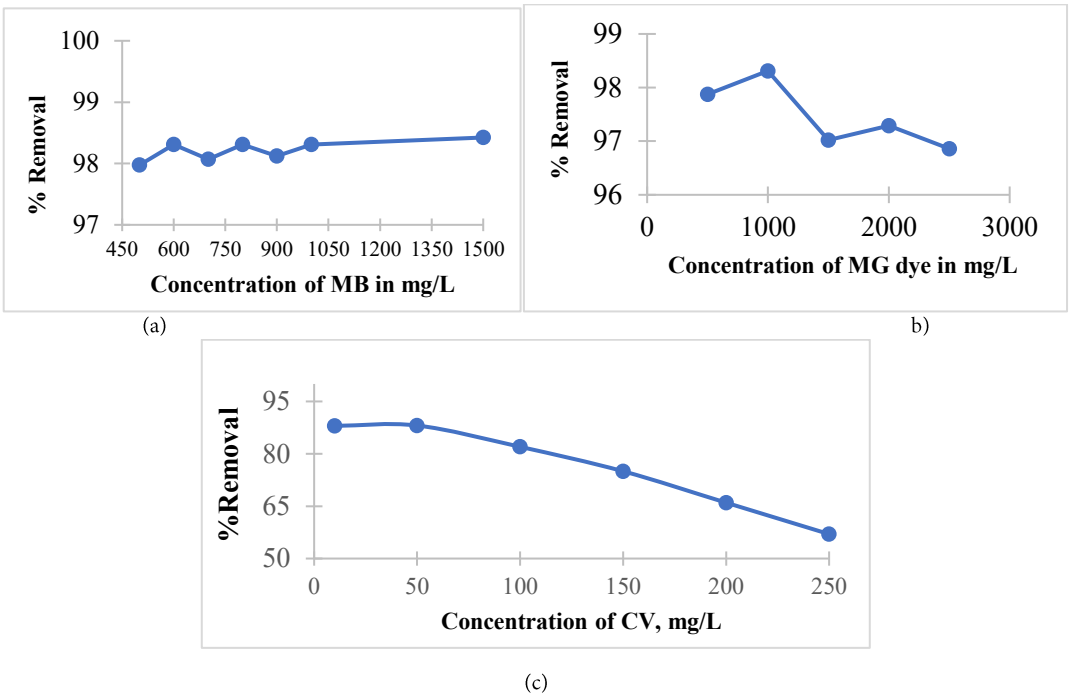

Fig. 5. Effect of concentration of (a) MB, (b) MG, and (c) CV on adsorption to 0.25 g of the active adsorbent at the flow rate of 1 mL/min at the operating pH of 2, 4.5, and 3, respectively, under the room temperature.

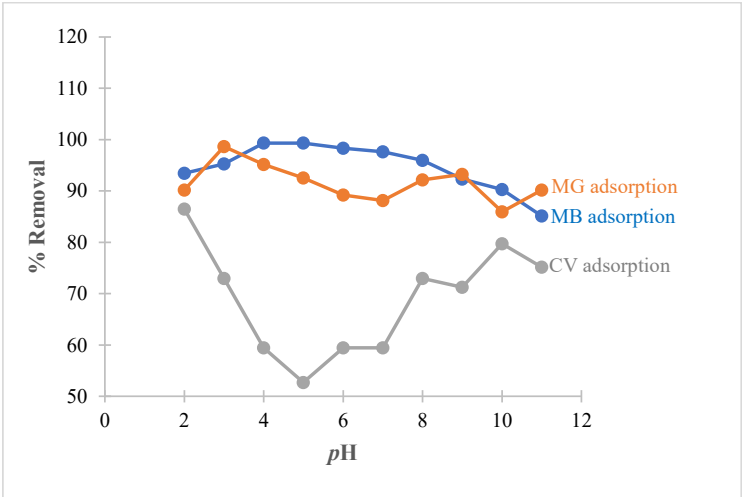

Fig. 6. Effect of pH on removal of MB, MG (both 1000 mg/L), and CV dye (50 mg/L) using 0.25 g of adsorbent at the operating pH of 2, 4.5, and 3, respectively for elution at a flow rate of 1mL/min under room temperature

Effect of contact time

Experiments were carried out to optimize the contact time at room temperature to obtain maximum dye removal. A 5 mL solution containing a specified concentration of CV (50 mg/L), MB, and MG (both 1000 mg/L) was eluted using a column filled with 0.25 g of adsorbent. The elution process was carried out after a residence time ranging from 2 to 20 minutes, and the removal rate was evaluated. The removal rate was found to be essentially stable throughout the various contact times examined. This shows that the contact period had a negligible effect on the dye removal.

Effect of Flow Rate

The effect of the flow rate of dye on removal

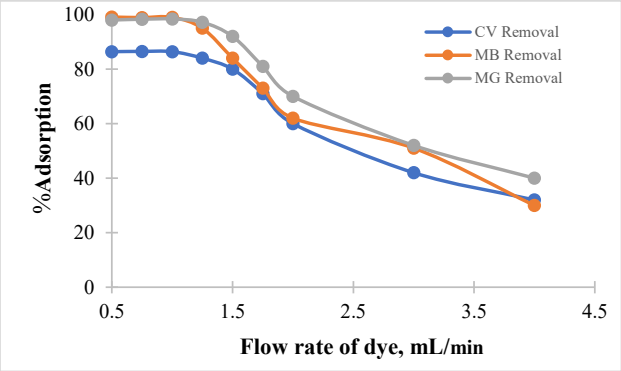

Fig. 7. Study of the effect of the flow rate of dye through the column for adsorption of MB, MG (800 mg/L), and CV (40 mg/L) on 0.25 g of activated husk at the operating pH of 2, 4.5, and 3, respectively under room temperature

efficiency was examined while keeping the adsorbent weight constant at 0.25 g. Flow rates ranging from 0.5 mL/min to 5 mL/min were evaluated. At the flow rates between 0.5 and 1.0 mL/min, an almost consistent percentage of adsorption of CV, MB, and MG was observed. According to the findings, as the flow rate increased, the proportion of dye elimination reduced. At greater flow rates, the contact period between the dye molecules and the adsorbent is shortened. We established that the optimized flow rate for the dye was 1 mL/min, as it was observed after careful consideration of the experimental findings. However, higher flow rates of 5 mL/min and above were found to make liquid elution through the column challenging. Fig. 7 depicts the fluctuations observed during the adsorption of CV, MB, and MG at various flow rates.

Chemical stability of adsorbent

The chemical stability of NaOH-LLPh was assessed across a range of organic and acidic solvents. This evaluation involved the use of solvent-washed and sun-dried material. The solvents employed in the treatment included methanol, ethanol, acetone, diethyl ether, methyl acetate, methyl benzoate, 0.1 M solutions of HCl, HNO_3, $HClO_4$, acetic acid, oxalic acid, and tartaric acid. The experimental investigation demonstrated that the adsorption capacity of NaOH-LLPh for MB, MG, and CV remained unaffected when utilizing the adsorbent treated with methanol, ethanol, acetone, diethyl ether, methyl acetate, methyl benzoate. The average percentage adsorption values for MB, MG, and CV on NaOH-LLPh post-treatment with the solvents were found to be 96.23, 97.52, and 87%, respectively, with corresponding relative standard deviations of 2.13, 1.89, and 1.88%. However, the adsorption capacity of NaOH-LLPh adsorbent treated with 0.1 M solutions of HCl, HNO_3, $HClO_4$, acetic acid, oxalic acid, and tartaric acid declined very marginally. The mean percent adsorption of MB, MG, and CV observed were 91.45, 86.45 and 81.26%, respectively. This provided conclusive evidence of the exceptional chemical stability of the adsorbent in these solvents.

Adsorption isotherm studies

Adsorption isotherm studies provide information on the interaction between adsorbent and adsorbate [73], as well as the underlying process. Attempts were made to investigate the adsorption of MB, MG, and CV on the adsorbent's surface. Adsorption isotherm analysis determines the relationship between the concentration and amount of dye accumulated on the surface of a certain amount of adsorbent under equilibrium conditions. To explain the adsorption process mathematically, the Langmuir and Freundlich adsorption isotherm models were used. According to the Langmuir isotherm model, the adsorbent surface is created with a single layer on the adsorbent's outer surface [43]. It confirms that the adsorbent surface has uniform adsorption sites, i.e., a homogeneous surface. Hence, the energy required for dye adsorption is uniform over the adsorbent's surface [73]. The Freundlich isotherm model, on the other hand, explains the non-uniform structure of the adsorbent's heterogeneous outer surface [67]. As a result, the energy required to adsorb the dye on the adsorbent's surface varies across the surface. The following is the mathematical expression for the Langmuir isotherm model [73]:

$$\frac{C_e}{q_e} = \frac{1}{bq_m} + \frac{C_e}{q_m} \quad (6)$$

Table 4. Separation constant (R_L) values for MB, MG, and CV adsorption at their different concentrations

MB		MG		CV	
Concentration of dye, mg/L	R_L (mg/L)	Concentration of dye, mg/L	R_L (mg/L)	Concentration of dye, mg/L	R_L (mg/L)
2500	0.04588	1000	0.07616	200	0.0106
2600	0.0442	1500	0.0521	400	0.0053
2700	0.04263	2000	0.03959	600	0.0035
2800	0.04117	2500	0.03192	800	0.0026
2900	0.03981	3000	0.02674	1000	0.0021
3000	0.03853	-	-	-	-

Table 5. Isotherm parameters for the adsorption of MB, MG, and CV

Dye	Isotherms	R^2	Parameters
MB	Freundlich	0.7254	n=1.92627, K_f= 3.1561 mg/g
	Langmuir	0.9910	b=0.00832, q_m=0.00034
MG	Freundlich	0.9729	n=8.86003, K_f= 2.3961 mg/g
	Langmuir	0.9958	b=0.01213, q_m=0.0002534
CV	Freundlich	0.7275	n=0.26130, K_f= 8.9892 mg/g
	Langmuir	0.6709	b=0.4726, q_m=0.01334

where C_e is the equilibrium concentration of dye (mmol/L), q_e is the amount of dye adsorbed per unit weight of adsorbent, q_m is the adsorption of dye on unit weight of adsorbent at a time (t) or adsorption capacity (mmol/g) or monolayer capacity. The terms b and q_m were determined from the intercept and slope of the C_e/q_e v/s C_e plot, respectively.

The mathematical equation for Freundlich isotherm model is given below [68]:

$$\log (q_e) = \log (k_f) + \log (C_e) / n \quad (7)$$

where k_f and n are empirical parameters that reflect sorption capacity and sorption intensity, respectively. These parameters are computed by plotting $\log(q_e)$ *versus* log(Ce). If 1/n is less than one, it implies normal adsorption; n = 1 indicates that the partition between the two phases is independent of concentration; and 1/n more than one shows cooperative adsorption.

The Langmuir isotherm was described in terms of a dimensionless constant called the separation factor (R_L), as indicated in the equation below [73]:

$$R_L = \frac{1}{(1+bC_0)} \quad (8)$$

where C_0 is the initial dye concentration and b is the Langmuir constant. The separation factors (R_L) are shown in Table 4. It is well understood that if the R_L value is more than one, adsorption is very low or negligible, R_L=1: adsorption is linear, and R_L<1: adsorption is outstanding. Tables 4 and 5 present the experimental outcomes of the study. Figs. 8 and 9 (provided as supplementary file: SF) show the experimental Langmuir and Freundlich adsorption isotherm graphs, respectively.

By analyzing the R^2 and R_L data in Tables 4 and 5, it is clear that MB and MG are well suited to the Langmuir isotherm model, but CV is well fitted with the Freundlich isotherm model.

Kinetics studies

The kinetic studies were carried out under optimal conditions, which included passing 1000 mg/L MB and MG dyes, and 50 mg/L CV through a 0.25g packed adsorbent column with a contact time ranging from 20 to 100 min, eluted at a flow rate of 1 ml/min, and taking absorbance measurements of the eluate. These investigations sought to study the dye's interaction with the adsorbent over time as well as its efficiency [44]. To undertake kinetic analyses on experimental data, mathematical equations were employed to determine the mechanism of adsorption and its rate-controlling or rate-determining steps, which can differentiate between mass transport and chemical reaction. Using experimental data,

Table 6. Results of pseudo-first-order model for adsorption of MB, MG, and CV on activated *Lablab purpureus* husk

Dyes	Concentration of dye, mg/L	q_e exp value, mg/L	k_1 in min^{-1}	q_e calc value, mg/L	R^2
MB	3000	1.17954	0.005169	0.41754	0.73454
MG	3000	2.508277	0.004276	0.27819	0.73688
CV	1000	4.093495	0.004445	0.471255	0.92821

Table 7. Results of the study of a pseudo-second-order model for MB, MG, and CV adsorption on activated *Lablab pupureus* husk

Dyes	Concentration of dye, mg/L	q_e exp value, mg/L	k_2 in min^{-1}	q_e calc value, mg/L	R^2
MB	3000	0.28082	1.679565	0.277846	0.999107
MG	3000	0.243583	0.000345	0.27819	0.999768
CV	1000	1.067744	0.019027311	0.471255	0.976855

pseudo-first order and pseudo-second order models were used to determine the kinetics of adsorption and this provided insights into the rate constants and mechanism. The regression coefficient or correlation coefficient (R^2) and experimental q_e values were used to determine the applicability of the kinetic models.

The following is the mathematical expression for the pseudo-first-order model [73]:

$$\log(q_e - q_t) = \log q_e - k_1 t \quad (9)$$

where q_e is the amount of dye adsorbed (mg/L) at equilibrium, q_t is the amount of solute adsorbed per unit weight of adsorbent at time t (mg/g), and k_1 is the rate constant for the pseudo first-order model. The graph of $\log(q_e\text{-}q_t)$ against t can be used to find the values of k_1 and q_e using slope and intercept, respectively. Table 6 displays the findings of these studies.

The following is a mathematical representation of the pseudo-second-order model [73]:

$$\frac{t}{q_t} = \frac{1}{k_2 q_e^2} + tq_e \quad (10)$$

where k_2 is the pseudo-second-order model's rate constant. The slope and intercept of t/q_t versus t graph were used to derive the values of k_2 and q_e, respectively. Fig. 10 and 11 (in SF) depict the corresponding kinetic models. Table 7 summarises the acquired results of this study.

The experimental data reported in Tables 6 and 7 for k_1, k_2, and R^2 indicate that the adsorption of MB, MG, and CV dyes followed the pseudo-second-order kinetics model.

Application to removal of dyes from spiked industrial effluent samples

The proposed adsorbent was employed to extract CV, MB, and MG from industrial effluent water samples spiked with known amounts of standard solutions. Table 8 shows the percentage of dye estimated after adsorption. The results show that utilizing NaOH-LLPh adsorbent, the dyes CV, MB, and MG can be removed up to 87.98%, 97.63%, and 99.10%, respectively.

Thermodynamic studies

The effect of temperature on the adsorption of MB, MG, and CV was studied. The MB and MG were taken at 600 mg/L and CV at 40 mg/L. The dye adsorption and elution procedure was performed for each dye separately at 298, 303, 308, and 313 K. The changes in Gibbs free energy (ΔG^0), entropy (ΔS^0), and enthalpy (ΔH^0) were determined [74] using the Van't Hoff equation. The results of thermodynamic studies are presented in Table 9. The results of negative ΔG^0 values and positive ΔH^0 values indicated the spontaneous endothermic process of adsorption.

Adsorption mechanism

The primary challenge in a study on adsorption lies in comprehending the adsorption mechanism. Nevertheless, before grasping this mechanism, it's essential to take into account two factors: firstly, the structure of the adsorbate, and secondly, the surface properties of the adsorbent. It's worth noting that MB, MG, and CV are cationic dyes containing amine groups within their composition. In aqueous solutions, the dyes dissociate into MB^+,

Table 8. Results of application of the proposed *Lablab purpureus* husk as adsorbent to remove MB, MG, and CV from spiked water samples (industrial effluents)

Dye	Concentration spiked, mg/L	Concentration found*±SD, mg/L	%Adsorption
MB	500.0	15.00±1.01	97.00
	600.0	21.60±0.89	96.40
	700.0	16.59±0.88	97.63
MG	500.0	04.50±1.56	99.10
	600.0	10.62±1.22	98.23
	700.0	12.74±0.97	98.18
CV	30.0	03.87±0.56	87.10
	40.0	04.81±0.61	87.98
	50.0	06.55±0.80	86.90

Injection volume 5 mL; Flow rate: 1 mL/min; Adsorbent dose: 0.25 g; Temperature 25 °C; Operating pH for MB, MG and CV are 2, 4.5 and 3, respectively.
*Mean value of three determinations

Table 9. Results of thermodynamic studies for adsorption of MB, MG, and CV on the adsorbent

Dye	Concentration, mg/L	Temperature, K	Change in Gibb's Free Energy, ΔG^0, kJ/mol	Change in standard entropy, ΔS^0, J/K/mol	Change in standard enthalpy, ΔH^0, kJ/mol
MB	600.0	298	-32.15	0.214988	31.96878
		303	-33.09		
		308	-34.25		
		313	-35.35		
MG	600.0	298	-33.16	0.204213	27.69451
		303	-34.18		
		308	-35.21		
		313	-36.22		
CV	40.0	298	-27.12	0.212105	36.068
		303	-28.22		
		308	-29.28		
		313	-30.30		

MG^+, CV^+ ions, and Cl^- ions [37, 61]. Treatment with NaOH alters the morphology of the adsorbent, eliminates hemicelluloses and lignin components, reduces silica content, and likely increases the crystallinity of the cellulose fraction. This may promote chemical interactions between the more exposed hydroxyl groups of the adsorbent and the dye ions. The mechanical bonding takes place more readily as the dye ions penetrate the adsorbent microstructure [37, 61].

Therefore, the adsorption of the studied dye onto the surface of the adsorbent, which is the NaOH-activated *Lablab Pupureus* husk (NaOH-LLPH), likely occurs because of the creation of surface hydrogen bonds between the hydroxyl groups of the sorbent and the nitrogen atoms within the dyes. The mechanism for a dye-hydrogen ion exchange process is outlined as follows [37, 61]:

NaOH-LLPH – OH = NaOH-LLPH – O^- + H^+

NaOH-LLPH – O^- + Dye^+ = NaOH-LLPH – O^- - Dye^+ + H^+.

CONCLUSION

The chroma trap procedure was used to remove three ionic organic dyes, CV, MB, and MG using a novel bio adsorbent, NaOH-activated *Lablab purpureus* husk, which is one of the most commonly available natural materials. Adsorption capacity was found to be increased in the alkali-treated adsorbent. The pictures of SEM analysis inferred the probable adsorption of dyes onto the surface of the natural biodegradable adsorbent. The adsorption surface and numerous parameters, including dye concentration, adsorbent dose, dye pH, contact time, and flow rate, were evaluated, and optimized, and were found free from complexities. The findings of Langmuir and Freundlich's adsorption isotherm experiments are described,

and they show that CV, MB, and MG adsorb well on the adsorbent. Kinetic studies revealed the pseudo-second-order adsorption model on the material. This first-ever and novel column chromatographic adsorption approach is found to be the most cost-effective way to remove CV, MB, and MG. The proposed adsorption method for spiked water samples produced outstanding findings that correlated with those that evolved to a greater degree of agreement. A comparative evaluation of the effectiveness of previously documented techniques for eliminating MB, MG, and CV using various husks as adsorbents has been carried out. As outlined in Table 1, it is clear that the use of NaOH-activated *Lablab purpureus* husk in this investigation surpasses other studies that employed different husks as adsorbents for the elimination of MB, MG, and CV. This superior performance can be attributed to its exceptional adsorption capacity, straightforward elution process, and uncomplicated removal mechanism. Despite recent advancements in the field of nanocomposites for sono-sorption [75, 76], this straightforward adsorption method for dye removal should be prioritized. This novel adsorbent holds promise for a wide range of industries seeking to remove harmful organic dyes from their wastewater.

CONFLICT OF INTEREST

The authors hereby declare that there is no conflict of interest.

REFERENCES

1. Celia, M.P and S. Suruthi, 2016. Textile Dye Degradation Using Bacterial Strains Isolated from Textile Mill Effluent. International Journal of Applied Research, 2 337-341.
2. Shindhal, T., P. Rakholiya, S. Varjani, A. Pandey, H. H. Ngo, W. Guo, H. Y. Ng and M. J. Taherzadeh, 2021. A Critical Review on Advances in the Practices and Perspectives for the Treatment of Dye Industry Wastewater. Bioengineered, 12: 70-87. https://doi.org/10.1080/21655979.2020.1863034
3. Adane, T., A. T. Adugna and E. Alemayehu, 2021. Textile Industry Effluent Treatment Techniques. Journal of Chemistry, 2021: 5314404. https://doi.org/10.1155/2021/5314404
4. Shokri, A., 2021. Using NiFe2O4 as a Nano Photocatalyst for Degradation of Polyvinyl Alcohol in Synthetic Wastewater. Environmental Challenges, 5: 100332. https://doi.org/10.1016/j.envc.2021.100332
5. Shokri, A., 2020. Using Mn Based on Lightweight Expanded Clay Aggregate (Leca) as an Original Catalyst for the Removal of NO2 Pollutant in Aqueous Environment. Surfaces and Interfaces, 21: 100705. https://doi.org/10.1016/j.surfin.2020.100705
6. Saghi, M., A. Shokri, A. Arastehnodeh, M. Khazaeinejad and A. Nozari, 2018. The Photo Degradation of Methyl Red in Aqueous Solutions by A-Fe2O3/SiO2 Nano Photocatalyst. Journal of Nanoanalysis, 5(3): 163-70. https://doi.10.22034/JNA.2018.543608.
7. Shokri, A., and M. S. Fard, 2023. Using α-Fe2O3/SiO2 as a Heterogeneous Fenton Catalyst for the Removal of Chlorophenol in Aqueous Environment: Thermodynamic and Kinetic Studies. International Journal of Environmental Science and Technology, 20: 383-396. https://doi.org/10.1007/s13762-022-04498-w
8. A. Shokri, 2022. Degradation of 4-Chloro Phenol in Aqueous Media Thru UV/Persulfate Method by Artificial Neural Network and Full Factorial Design Method. International Journal of Environmental Analytical Chemistry, 102(17): 5077-5091. https://doi.org/10.1080/03067319.2020.1791328
9. Adegoke, K. A., and O. S. Bello, 2015. Dye Sequestration using Agricultural Wastes as Adsorbents. Water Resources and Industry, 12: 8-24. https://doi.org/10.1016/j.wri.2015.09.002
10. Dassanayake, R. S., S. Acharya and N. Abidi, 2021. Recent Advances in Biopolymer-Based Dye Removal Technologies. Molecules, 26(15): 4697. https://doi.org/10.3390/molecules26154697
11. Al-Degs, S. Y., and A. J. Sweileh, 2012. Simultaneous Determination of Five Commercial Cationic Dyes in Stream Waters Using Diatomite Solid-Phase Extractant and Multivariate Calibration. Arabian Journal of Chemistry, 5(2): 219-224. https://doi.org/10.1016/j.arabjc.2010.08.016
12. Karić, N., A. S. Maia, A. Teodorović, N. Atanasova, G. Langergraber, G. Crini, A. R. L. Ribeiro and M. Đolić, 2022. Bio-Waste Valorisation: Agricultural Wastes as Biosorbents for Removal of (In)Organic Pollutants in Wastewater Treatment. Chemical Engineering Journal Advances, 9: 100239. https://doi.org/10.1016/j.ceja.2021.100239
13. Namasivayam, C., D. Sangeetha and R. Gunasekaran, Removal of Anions, 2007. Heavy Metals, Organics and Dyes from Water by Adsorption onto a New Activated Carbon from Jatropha Husk, An Agro-Industrial Solid Waste. Process Safety and Environmental Protection, 85: 181-184. https://doi.org/10.1205/psep05002
14. Aryee, A.A., R. Zhang, H. Liu, R. Han, Z. Li and L. Qu, 2020. Application of Magnetic Peanut Husk for Methylene Blue Adsorption in Batch Mode. Desalination and Water Treatment, 194: 269-279. https://doi.org/10.5004/dwt.2020.25862
15. Ibrahim, A. A., E. A. Zayid, S. A. Dhikeel and M. Y. Najem, 2022. Biosorption Removal of Methylene Blue Dye from Aqueous Solutions using Phosphoric Acid-Treated Balanites Aegyptiaca Seed Husks Powder. Biointerface Research in Applied Chemistry, 12(6): 7845-7862. https://doi.org/10.33263/BRIAC126.78457862
16. Ashrafi, S. D., H. Kamani and A. H. Mahvi, 2016. The Optimization Study of Direct Red 81 and Methylene Blue Adsorption on NaOH-Modified Rice Husk. Desalination and Water Treatment, 57(2): 738-746. https://doi.org/10.1080/19443994.2014.979329
17. Abhay, P. R., V. Kumar and D. P. Singh, 2020. A Combined Effect of Adsorption and Reduction Potential of Biochar Derived from Mentha Plant Waste on Removal of Methylene Blue Dye From Aqueous Solution. Separation Science and Technology, 55(5): 907-921. https://doi.org/10.1080/01496395.2019.1580732
18. Pankaj, S., R. Kaur, C. Baskar and W-J. Chung, 2010.

Removal of Methylene Blue from Aqueous Waste using Rice Husk and Rice Husk Ash. Desalination, 259(1-3): 249-257. https://doi.org/10.1016/j.desal.2010.03.044

19. Leshan, U., C. Thambiliyagodage, R. Wijesekera and M. G. Bakker, 2021. Synthesis of Mesoporous Silica Nanoparticles Derived from Rice Husk and Surface-Controlled Amine Functionalization for Efficient Adsorption of Methylene Blue from Aqueous Solution. Current Research in Green and Sustainable Chemistry, 4: 100116. https://doi.org/10.1016/j.crgsc.2021.100116
20. Weihua, Z., K. Li, H. Bai, X. Shi and R. Han, 2011. Enhanced Cationic Dyes Removal from Aqueous Solution by Oxalic Acid Modified Rice Husk. Journal of Chemical Engineering Data 56(5): 1882. https://doi.org/10.1021/je100893h
21. Praveen, S., J. Josephraj, B. P. Thillainayagam and G. Ravindiran, 2023. Evaluation of the Adsorptive Removal of Cationic Dyes by Greening Biochar Derived from Agricultural Bio-Waste of Rice Husk. Biomass Conversion Biorefinery, 13: 4047-4060. https://doi.org/10.1007/s13399-021-01415-y
22. Sharma, Y. C., Uma and S. N. Upadhyay, 2011. An Economically Viable Removal of Methylene Blue by Adsorption on Activated Carbon Prepared from Rice Husk. The Canadian Journal of Chemical Engineering, 89(2): 377-383. https://doi.org/10.1002/cjce.20393
23. Stevens, A. O., U. N. Emeh and N. O. Eddy, 2018. Experimental and Computational Chemistry Studies on the Removal of Methylene Blue and Malachite Green Dyes from Aqueous Solution by Neem (Azadirachta Indica) Leaves. Journal of Taibah University for Science, 12(3): 255-265. https://doi.org/10.1080/16583655.2018.1465725
24. Thi, H. T., H.H. Le, T. H. Pham, D. T. Nguyen, D.D. La, S.W. Chang, S.M. Lee, W.J. Chung and D.D. Nguyen, 2021. Comparative Study on Methylene Blue Adsorption Behavior of Coffee Husk-Derived Activated Carbon Materials Prepared using Hydrothermal and Soaking Methods. Journal of Environmental Chemical Engineering. 9(4): 105362. https://doi.org/10.1016/j.jece.2021.105362
25. Karaçetin, G., S. Sivrikaya and M. Imamotlu, 2014. Adsorption of Methylene Blue from Aqueous Solutions by Activated Carbon Prepared from Hazelnut Husk Using Zinc Chloride. Journal of Analytical and Applied Pyrolysis, 110(1): 270-276. https://doi.org/10.1016/j.jaap.2014.09.006
26. Mohd, A. A., B. A. Nur'Adilah, A. A. Kayode and S. B. Olugbenga, 2019. Sorption Studies of Methyl Red Dye Removal Using Lemon Grass (Cymbopogon Citratus). Chemical Data Collections, 22: 100249. https://doi.org/10.1016/j.cdc.2019.100249
27. Shubhada, S. N., N. A. Mirgane, V. S. Shivankar, K.B. Pathade and G.C. Wadhawa, 2020. Adsorption of Methylene Blue Dye Over Activated Charcoal from the Fruit Peel of Plant Hydnocarpus Pentandra. Materials Today Proceedings, 37: 2302-2305. https://doi.org/10.1016/j.matpr.2020.07.728
28. Amanda, R., O. Pezoti, L. S. Souza, I.P.A.F. Souza, K. C. Bedin, P. S. C. Souza, T. L. Silva, S. A. R. Melo, A. L. Cazetta and V. C. Almeida, 2017. Hydrothermal Carbonization of Coffee Husk: Optimization of Experimental Parameters and Adsorption of Methylene Blue Dye. Journal of Environmental Chemical Engineering, 5(5): 4841-4849. https://doi.org/10.1016/j.jece.2017.08.035
29. Warda, H., U. Farooq, M. Ahmad, M. Athar and M.A. Khan, 2017. Potential Biosorbent, Haloxylon Recurvum Plant Stems, for the Removal of Methylene Blue Dye. Arabian Journal of Chemistry, 10: S1512. https://doi.org/10.1016/j.arabjc.2013.05.002
30. Indrajit, G., S. Kar, T. Chatterjee, N. Bar, S.K. Das, 2021. Removal of Methylene Blue from Aqueous Solution using Lathyrus Sativus Husk: Adsorption Study, MPR and ANN Modelling. Process Safety and Environmental Protection, 149: 345-361. https://doi.org/10.1016/j.psep.2020.11.003
31. Chosel, P. L and R. E. C. Amon, 2020. Magnetic Rice Husk Ash "Cleanser" as Efficient Methylene Blue Adsorbent. Environmental Engineering Research, 25(5): 685-692. https://doi.org/10.4491/eer.2019.287
32. Anees, A., N. Khan, B.S. Giri, P. Chowdhary and P. Chaturvedi, 2020. Removal of Methylene Blue Dye Using Rice Husk, Cow Dung and Sludge Biochar: Characterization, Application, and Kinetic Studies, Bioresource and Technology, 306: 123202. https://doi.org/10.1016/j.biortech.2020.123202
33. Oana, M. P., C. Pecurariu and S. G. Muntean, 2014. Kinetic and Thermodynamic Studies on Methylene Blue Biosorption using Corn-Husk, Royal Society of Chemistry, 4(107): 62621-62630. https://doi.org/10.1039/C4RA10504D
34. Kruti, V and D. Dharajiya, 2019. Adsorptive Removal of Six Dyes from Aqueous Solution using Normal and Modified Sawdust of Gmelina Arborea Roxb. International Journal of Pharmacy and Biological Sciences, 9(2): 179-186. https://doi:10.21276/ijpbs.2019.9.2.25
35. Gobi, K., M. D Mashitah and V. M. Vadivelu, 2011. Adsorptive Removal of Methylene Blue using a Novel Adsorbent from Palm Oil Mill Effluent Waste Activated Sludge: Equilibrium, Thermodynamics, and Kinetic Studies. Chemical Engineering Journal, 171(3): 1246-1252. https://doi.org/10.1016/j.cej.2011.05.036
36. Siji, C., S. Tang, Y. Sun, G. Wang, H. Chen, X. Yu, Y. Su and G. Chen, 2018. Preparation of a Highly Porous Carbon Material Based on Quinoa Husk And its Application for Removal of Dyes by Adsorption. Materials (Basel), 11(8): 1407. https://doi.org/10.3390/ma11081407
37. Binod, K and U. Kumar, 2015. Adsorption of Malachite Green in an Aqueous Solution Onto Sodium Carbonate Treated Rice Husk. Korean Journal of Chemical Engineering, 32(8): 1655-1666. https://doi.org/10.1007/s11814-014-0351-5
38. Adugna, N. A., G. Y. Abate and A. T. Habte, 2020. Bioadsorption of Basic Blue Dye from Aqueous Solution onto Raw and Modified Waste Ash as Economical Alternative Bioadsorbent, Journal of Chemistry, 2020: Article ID: 8746035. https://doi.org/10.1155/2020/8746035
39. Malik, R., D.S. Ramteke and S.R. Wate, 2007. Adsorption of Malachite Green on Groundnut Shell Waste Based Powdered Activated Carbon, Waste Management, 27(9): 1129-1138. https://doi.org/10.1016/j.wasman.2006.06.009
40. Abdoulaye, D. N., Y.A.E.H. Ali, O.E.M. Abdallahi, M.A. Bollahi, M. Stitou, M. Kankou and D. Fahmi, 2020. Sorption of Malachite Green from Aqueous Solution using Typha Australis Leaves as a Low-Cost Sorbent. Journal of Environmental Treatment Techniques, 8(3): 1023-1028.
41. Mohd, A. A., N. Ahmad and O. S. Bello, 2014. Adsorptive Removal of Malachite Green Dye using Durian Seed-Based Activated Carbon. Water Air Soil Pollution, 225(8): 2057. https://doi.org/10.1007/s11270-014-2057-z
42. Ravikumar, M and E. G. Aklilu, 2017. A Comparative Study on Removal of Malachite Green Dye from Waste Water

using Different Low Cost Adsorbents, International Journal of Engineering Research and Technology, 6(04): 262. https://doi.org/10.17577/IJERTV6IS040338

43. Farnaz, H., R. Norouzbeigi, F. Sarbisheh and H. Shayesteh, 2016. Malachite Green Removal using Modified Sphagnum Peat Moss as A Low-Cost Biosorbent: Kinetic, Equilibrium, and Thermodynamic Studies, Journal of Taiwan Institute of Chemical Engineers, 58: 482-489. https://doi.org/10.1016/j.jtice.2015.07.004
44. Manoj, D and C. Mishra, 2019. Jackfruit Leaf as an Adsorbent of Malachite Green: Recovery and Reuse of the Dye, SN Applied Science. 1(5): 483. https://doi.org/10.1007/s42452-019-0459-7
45. Arora, V and D. P. Tiwari, 2020. Remediation of Colour Pollutant Malachite Green Dye with Mesoporous Walnut Based Particles as Efficient Adsorbent: Isotherms, Kinetics and Batch Adsorption Equilibrium Study. Indian Journal of Environmental Protection, 40(3): 227-234.
46. Hejun, R., R. Zhang, Q. Wang, H. Pan and Y. Wang, 2016. Garlic Root Biomass as Novel Biosorbents for Malachite Green Removal: Parameter Optimization, Process Kinetics and Toxicity Test. Chemical Research in Chinese Universities, 32(4): 647-654. https://doi.org/10.1007/s40242-016-6095-5
47. Fouzia, M and A. Nasar, 2019. Preparation, Characterization, and Adsorption Studies of the Chemically Modified Luffa Aegyptica Peel as a Potential Adsorbent for the Removal of Malachite Green from Aqueous Solution. Journal of Molecular Liquids, 274: 315-327. https://doi.org/10.1016/j.molliq.2018.10.119
48. Arpita, G., 2021. Application of Cocos Nucifera's Husk to Remove Malachite Green Dye and Response Surface Modeling. Bulgarian Chemical Communications, 53: 44. https://doi:10.34049/bcc.53.D.28
49. Neetu, S., D. P. Tiwari and S. K. Singh, 2020. Sorption Potential of Treated Plant Residues viz. Potato Peel and Neem Bark for Removal of Synthetic Dyes from Aqueous Solution. Rasayan Journal of Chemistry, 13(2): 1063-1073. https://doi.org/10.31788/RJC.2020.1325405
50. Mohamad, F. M. Y., M. A. Ahmad, N. A. Rosli, F. N. Gonawan and S. J. Abdullah, 2021. Scavenging Malachite Green Dye from Aqueous Solution using Durian Peel Based Activated Carbon. Malaysian Journal of Fundamental and Applied Sciences, 17(1): 95. https://doi.org/10.11113/mjfas.v17n1.2173
51. Mouhammad, H., P. Parthasarathy, H. R. Mackey, T. Al-Ansari and G. McKay, 2021. Minimizing Adsorbent Requirements using Multi-Stage Batch Adsorption for Malachite Green Removal using Microwave Date-Stone Activated Carbons. Chemical Engineering and Processing - Process Intensification, 167: 108318. https://doi.org/10.1016/j.cep.2021.108318
52. Dilli, D and P. L. Homagai, 2020. Adsorptive Removal of Malachite Green Dye from Aqueous Solution using Chemically Modified Charred and Xanthated Wheat Bran. Journal of Nepal Chemical Society, 41(1): 103-109. https://doi.org/10.3126/jncs.v41i1.30495
53. Vijayalakshmi, G and S. Sivajiganesan, 2020. Removal of Malachite Green Dye by Teak Wood Waste Biomass Activated Carbon and its Antimicrobial Activity. European Journal of Medicinal Plants, 31(6): 18-25. https://doi.org/10.9734/ejmp/2020/v31i630244
54. Sudarni, D. H. A., U. O. Aigbe, K. E. Ukhurebor, R. B. Onyancha, H. S. Kusuma, H. Darmokoesoemo, O. A. Osibote, V. A. Balogun and B. A. Widyaningrum, 2021. Malachite Green Removal by Activated Potassium Hydroxide Clove Leaf Agrowaste Biosorbent: Characterization, Kinetic, Isotherm, and Thermodynamic Studies. Adsorption Science and Technology, 2021: Article 1145312 https://doi.org/10.1155/2021/1145312
55. Bamgbose, J. T., B. A. Adesina, N. M. Olubunmi, A. S. Akinyeye and I. A. Ayodeji, 2012. Kinetics and Thermodynamic Studies of Adsorption of Malachite Green onto Unmodified and EDTA-Modified Groundnut Husk. African Journal of Pure and Applied Chemistry, 6(14): 141. https://doi:10.5897/AJPAC12.047
56. Chrispine, M. O., J. M. Onyari, W. C. Wanyonyi, J. N. Wabomba and V. M. Muinde, 2020. Adsorptive Removal of Hazardous Crystal Violet Dye from Aqueous Solution using Rhizophora Mucronata Stem-Barks: Equilibrium and Kinetics Studies. Environmental Chemistry and Ecotoxicology, 2: 64-72. https://doi.org/10.1016/j.enceco.2020.05.001
57. Khoiria, N. A. P., S. Kaewpichai, A. Keereerak and W. Chinpa, 2021. Facile Green Preparation of Lignocellulosic Biosorbent from Lemongrass Leaf for Cationic Dye Adsorption. J Pol Env. 29(6): 1681-1693. https://doi.org/10.1007/s10924-020-02001-5
58. Ashish, K. N and A. Pal, 2021. Enhanced Adsorption of Gentian Violet Dye from Water using Lignocellulosic Agricultural Waste Modified With Di- and Tri-Carboxylic Acids: Artificial Intelligence Modeling, Practical Comprehension, Mechanistic And Regeneration Analyses. Journal of Environmental Chemical Engineering, 9(4): 105578. https://doi.org/10.1016/j.jece.2021.105578
59. Sumanjit, K., S. Rani and R. K. Mahajan, 2015. Adsorptive Removal of Dye Crystal Violet onto Low-Cost Carbon Produced from Eichhornia Plant: Kinetic, Equilibrium, and Thermodynamic Studies. Desalination and Water Treatment, 53(2): 543-556. https://doi.org/10.1080/19443994.2013.841109
60. Sagnik, C., S. Chowdhury and P. D. Saha, 2013. Response Surface Optimization of a Dynamic Dye Adsorption Process: A Case Study of Crystal Violet Adsorption onto NaOH-Modified Rice Husk. Environmental Science and Pollution Research, 20(3): 1698-1705. https://doi.org/10.1007/s11356-012-0989-7
61. Sagnik, C., S. Chowdhury and P. D. Saha, 2011. Adsorption of Crystal Violet from Aqueous Solution onto NaOH-Modified Rice Husk. Carbohydrate Polymers, 86(4): 1533-1541. https://doi.org/10.1016/j.carbpol.2011.06.058
62. Babalola, A. O., O. C. Olawole, A. O. Ayeni and S. E. Sanni, 2020. African Star Apples Whole Seed Activated Carbon Powder as a Bio-Adsorbent of Crystal Violet Dye Removal from Aqueous Solution. Water Conservation Science and Engineering, 5(1-2): 97-114. https://doi.org/10.1007/s41101-020-00088-4
63. Satyaprasad, Y., A. I. Raju Ch and R. P. Jaganada, 2020. Isothermal and Kinetics of Biosportion Capacity of Crystal Violet Dye by using Red Algae Gelidium Pusillum, Journal of Critical Reviews, 7(05): 2477-2493.
64. Hira, U., T. Javed, M. B. Taj and M. N. Haider, 2023. Adsorption of Crystal Violet Dye from Wastewater on Phyllanthus Emblica Fruit (PEF) Powder: Kinetic and Thermodynamic. International Journal of Environmental Analytical Chemistry, 1: In Press. https://doi.org/10.1080/03067319.2023.2176229

65. Youssef, H. M., S. M. El-Dafrawy, E. A. Badran and M. M. El-Defrawy, 2022. Adsorptive Performance of Chemically Treated Olive Pomace for the Removal of Crystal Violet from Aqueous Solutions: Characterisation, Optimisation, Regeneration and Isotherm Studies. International Journal of Environmental Analytical Chemistry 102(19): 8019-8036. https://doi.org/10.1080/03067319.2020.1843647
66. Aljeboree, A. M and A. F. Alkaim, 2019. Role of Plant Wastes as an Ecofriendly for Pollutants (Crystal Violet Dye) Removal from Aqueous Solutions. Plant Achieves, 19: 902-905.
67. Sumaira, B., R. Rehman, T. Mahmud, S. Basharat and L. Mitu, 2020. Tartaric Acid-Modified Holarrhena Antidysenterica and Citrullus Colocynthis Biowaste for Efficient Eradication of Crystal Violet Dye from Water. Journal of Chemistry, 2020: Article ID 8862167. https://doi.org/10.1155/2020/8862167
68. Garmia, D and H. Zaghouane-Boudiaf, 2019. Urtica Dioica Leaves-Calcium Alginate as a Natural, Low-Cost, and Very Effective Bioadsorbent Beads in the Elimination of Dyes from an Aqueous Medium: Equilibrium Isotherms and Thermodynamic Studies, International Journal of Biological Macromolecules, 124: 915-921. https://doi.org/10.1016/j.ijbiomac.2018.11.253
69. Mauro C de, C. G., C. V. A. Carla, J. F. C. Jaciene, A. A. S. Sirlane, S. S. Hildo A dos, M. M. Suzyeth, F. Robson and W. B. B. Cícero, 2019. Expressive Removal Of Cationic Dyes (Methylene Blue and Crystal Violet) by Carnauba Straw (Copernicia Cerifera), The Pharmaceutical and Chemical Journal, 6(3): 37-52.
70. Koushik, G., N. Bar, A. B. Biswas and S. K. Das, 2021. Elimination of Crystal Violet from Synthetic Medium by Adsorption using Unmodified and Acid-Modified Eucalyptus Leaves with MPR and GA Application. Sustainable Chemistry and Pharmacy, 19: 100370. https://doi.org/10.1016/j.scp.2020.100370
71. Hassanien, G., E. M. A. El-Monaem, A. S. Eltaweil and A. M. Omer, 2022. Efficient Removal of Noxious Methylene Blue and Crystal Violet Dyes at Neutral Conditions by Reusable Montmorillonite/NiFe2O4@Amine-Functionalized Chitosan Composite. Scientific Reports, 12(1): 15499. https://doi.org/10.1038/s41598-022-19570-1
72. Brini, L., A. Hsini, Y. Naciri, A. Bouziani, Z. Ajmal, K. H'Maida, A. Boulahya, M. Arahou, B. Bakiz, A. Albourine and M. Fekhaoui, 2021. Synthesis and Characterization of Arginine-Doped Heliotrope Leaves with High Clean-Up Capacity for Crystal Violet Dye from Aqueous Media. Water Science and Technology. 84: 2265-2277. https://doi.org/10.2166/wst.2021.446
73. Alene, A. G., G. Y. Abate and A. T. Habte, 2020. Bioadsorption of Basic Blue Dye from Aqueous Solution onto Raw and Modified Waste Ash as Economical Alternative Bioadsorbent. Journal of Chemistry, 2020: Article ID 8746035. https://doi.org/10.1155/2020/8746035
74. Gavioli, E., N. M. Maier, K. Haupt, K. Mosbach and W. Lindner, 2005. Analyte Templating: Enhancing the Enantioselectivity of Chiral Selectors upon Incorporation Into Organic Polymer Environments. Analytical Chemistry, 77: 5009-5018. https://doi.org/10.1021/ac050407s
75. Eizi, R., T. R. Bastami, V. Mahmoudi, A. Ayati and H. Babaei, 2023. Facile Ultrasound-Assisted Synthesis of CuFe-Layered Double Hydroxides/g-C3N4 Nanocomposite for Alizarin Red S Sono-Sorption. Journal of the Taiwan Institute of Chemical Engineers, 145: 104844. https://doi.org/10.1016/j.jtice.2023.104844
76. Najafi, M., T. R. Bastami, N. Binesh, A. Ayati and S. Emamverdi, 2022. Sono-sorption versus Adsorption for the Removal of Congo Red from Aqueous Solution using NiFeLDH/Au Nanocomposite: Kinetics, Thermodynamics, Isotherm Studies, and Optimization of Process Parameters. Journal of Industrial and Engineering Chemistry, 116: 489-503. https://doi.org/10.1016/j.jiec.2022.09.039